

SIMULATING CANOPY GAP FRACTION OF COMPLEX 3D FOREST SCENES OF *PICEA SITCHENSIS* (SITKA SPRUCE)

M. Pfeifer^{1,2}, M. Disney², P. Lewis²

1. Institute of Vegetation Ecology and Nature Conservation (VegNat), Potsdam University, Maulbeerallee 2, 14469 Potsdam, Germany, marion.pfeifer@googlemail.com

2. Department of Geography, University College London, Gower St., London WC1E 6BT, and NERC Centre for Terrestrial Carbon Dynamics, mdisney@geog.ucl.ac.uk, plewis@geog.ucl.ac.uk

KEY WORDS: Forestry; 3D canopy modelling; gap fraction; hemispherical photography.

ABSTRACT:

We present an application of 3D canopy modelling for assessing the structural accuracy of complex 3D structural models of Sitka spruce. Such models can be used to simulate canopy reflectance at the landscape-scale with a minimum number of assumptions. Typically, however, the underlying canopy structural models require a large number of parameters, many of which are hard to measure and so must be estimated. How then can the resulting canopy structure be validated? We compare estimates of canopy gap fraction of modelled Sitka spruce from simulating hemispherical canopy reflectance from within the canopy, with those derived from upward-looking hemispherical photography from Harwood Forest, Northumberland, UK. Results show that gap fraction estimated from the 3D model canopies compares well with estimates derived from hemispherical photography. Where estimates disagree, such comparisons can be used to inform improvement of the structural models. We also use the detailed structural models to explore the sensitivity of hemispherical photography methods to error in estimating gap fraction in the field.

1. INTRODUCTION

Forest ecosystems and their interactions with the atmosphere, both as a sink and a source of carbon, are vital systems to study when estimating terrestrial carbon budgets (Dixon et al. 1994, Carrara et al. 2003) and ecosystem productivity (Schulze et al. 1999, Reich & Bolstad 2001). The structure of the forest canopy, especially the vertical and spatial distribution, orientation, and density of foliage and its supporting structures, plays a crucial role determining patterns of carbon exchange and nutrient cycling in the canopy, particularly via radiation interception (Ross 1981, Widlowski et al. 2004).

Canopy structure i.e. the size and distribution of canopy elements (and their optical properties), is complex, spatially heterogeneous, and temporally variable (Weiss et al. 2004). This makes accurate ground-based measurements of biophysical parameters such as the leaf area index (LAI) and the fraction of absorbed photosynthetically active radiation (fAPAR) over larger areas time-consuming and expensive. Thus, research has focussed on algorithms permitting the derivation of biophysically relevant parameters from remotely sensed data (Price 1993, Sellers et al. 1994, Myneni et al. 1997), thereby providing the potential for monitoring the photosynthetic activity of terrestrial ecosystems at regional and global scales at daily time intervals (Deng et al. 2006). Such algorithms can be based on 1D and 3D radiation transfer models (Knyazikhin et al. 1998, Myneni et al. 2002, Pinty et al. 2006), which are capable of simulating radiation scattering and absorption of vegetation stands.

More recently, dynamic structural models for the growth of vegetation structure have been generated to improve the reliability of quantitative parameter estimation from satellite images (Saich et al. 2003, Disney et al. 2006). By simulating the reflectance and scattering of highly-

detailed 3D structural models of forest canopies, look-up-tables (LUTs) can be generated describing the relationship between canopy architecture and measured reflectance using a minimum number of simplifying assumptions. However, the underlying 3D structural models require a large number of parameters, many of which are often unavailable or too time-intensive to be measured in practice, which must be estimated.

Digital hemispherical photography may be a suitable tool to validate canopy structure in 3D models of vegetation structure. Hemispherical photography has been shown to be the ideal tool for studying plant canopy architecture and estimating the gap fraction in real forest stands providing information on size and density of gaps in the canopy rapidly and cheaply (reviewed in Jonckheere et al. 2004).

We simulate hemispherical reflectance from within the canopy of 3D structural forest models, and compare estimates of gap fraction derived from such simulations with estimates of gap fraction derived from upward-looking digital hemispherical photography acquired in Sitka spruce (*Picea sitchensis* (Bong.) Carr.) forest stands at Harwood Forest (Northumberland, UK). We ask the following questions:

- (1) Can we validate modelled 3D forest structure of *Sitka spruce* forest stands by comparing simulations of hemispherical reflectance of 3D models with hemispherical images required in-situ?
- (2) What is the impact on estimates of gap fraction / structure derived from hemispherical photography of: camera location (sampling frequency, proximity to trees), camera attitude, and focus. What are the implications of violating assumptions of leaf angle variability, clumping, etc on estimates of LAI derived from hemispherical photography?

2. MATERIAL AND METHODS

2.1 3D modelling of Sitka spruce canopies

We developed realistic detailed 3D structural models of Sitka spruce forest canopies in order to simulate reflectance values measured remotely (following the method of Disney et al. 2006). The mechanistic *Treegrow* model (developed from the PINOGRAM model of Leersnijder 1992, Oevelen van & Woodhouse IH 1996), an existing structural growth model of *Pinus sylvestris* L., was modified and used to generate trees for six age classes (5, 9, 12, 20, 30, and 40 years) of Sitka spruce. *Treegrow* is an empirical growth model which is parameterised by species- and site-specific empirical height and branching functions. By varying the seed for the pseudo-random number generator, five individual trees were generated per age class. These were then used for modelling forest stands permitting some tree level variability within each age class (Saich et al. 2003). Tree height was modified outside *Treegrow* to mimic observed height variation. The light extinction function implemented in *Treegrow* describes the variation with age of the percentage of light reaching the ground from the top of the canopy, and thereby determines the shape of the tree crown. The site-specific light extinction function was iteratively validated by simulating the light reduction through tree crowns, comparing resultant modelled and in-situ observed tree crown shape, and ground- to - crown heights, updating the function and when re-simulating (Disney et al. 2006). The modelled trees were validated by visual estimation (crown shape) and by comparing tree traits modelled with tree traits measured (e.g. height, diameter-at-breast height dbh, Fig. 1).

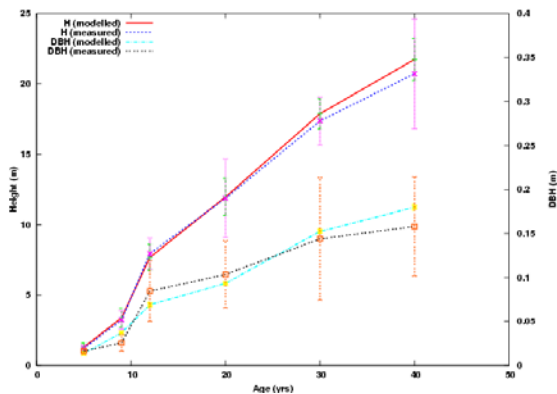


Figure 1. Tree height dbh modelled and measured at Harwood forest as a function of tree age.

Modelled trees were planted in age-specific forest stands according to measurements of tree spacing made at Harwood Forest. The observed forest stands are planted at high density and in a regular pattern causing deep shade in older forest stands and larger height-to-crown values (Fig. 2). Management at the site includes thinning to optimise growth conditions for all trees in the forest stand.

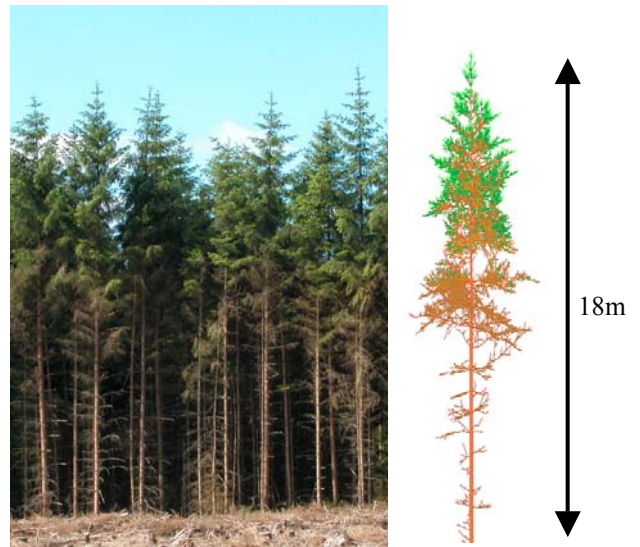


Figure 2. Left: Picture of a 30 years old forest stand of Sitka spruce taken at the Harwood Forest field site. Right: Model of a 30 years old Sitka spruce tree created with *Treegrow*.

The modelled forest stands were generated to be 300m on a side, and only the central 50 m x 50 m region was viewed in simulations to avoid edge effects (Saich et al. 2003). Because leaves are not included in the *Treegrow* model, they have been added here to the branches of the modelled trees using species- and site-specific measurements on needle size and density, and needle distribution (based on literature, Chandler & Dale 1990). The total length of green branches was obtained from the *Treegrow* derived tree model (Woodhouse & Hoekman 2000).



Figure 3. Model of a 9 yrs old Sitka spruce tree with needles. Needles were added to the “green” branches according to a Fibonacci distribution. Mean needle density and mean needle length were derived from field measurements.

2.2 Analysis of hemispherical images via CanEye

Hemispherical photographs were recorded in 5, 9, 12, 20, 30, and 40 years old forest stands of Sitka spruce in Harwood Forest in 2003 using a Nikon Coolpix 5000 with 180° fisheye adaptor. Hemispherical reflectance was simulated from within the forest models using a Monte Carlo ray tracing model (based on the *drat* model of Lewis, 1999) mimicking the properties of upward-looking hemispherical photography. Images were created for subsequent analysis using the CanEye software (version 4.1, Baret F. 2007: http://www.avignon.inra.fr/can_eye/). Image generation was only carried out as part of the “Transect” experiment (see below). In the other experimental cases (where gap fraction was sampled from multiple locations rather than from a single point) image generation was not appropriate.

In-situ hemispherical photographs (Fig. 4) were “thresholded” classifying pixels into vegetation / non-vegetation via an iterative algorithm that searches for the optimal threshold value (Ridler & Calvard 1978, Magid et al. 1990).

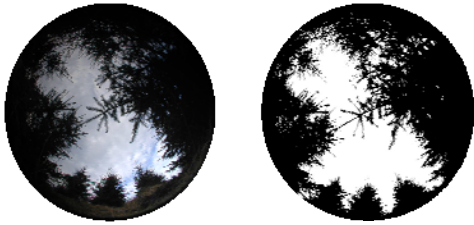


Figure 4. Hemispherical photograph of the 9 years old Sitka spruce forest stands before (left) and after (right) the “thresholding” procedure.

The leaf area index (LAI), defined as one half the total leaf area per unit ground surface area to account for irregular and non-flat forms of leaves (Chen & Black 1991, Fassnacht et al. 1994, Stenberg et al. 1994), is a critical parameter in studies of atmosphere-vegetation interaction and in models of vegetation canopy response to environmental changes (Deng et al. 2006). LAI estimates (LAI_{57} , LAI_{eff} , LAI_{true}) and gap fraction probability as a function of zenith angle were automatically derived from the “thresholded” images using CanEye. LAI_{57} is derived at a view zenith angle of 57.5°, which is suggested to be almost independent of foliage inclination angle (Warren-Wilson 1963). Effective LAI (LAI_{eff}) is directly retrieved by model inversion in CanEye based on a Poisson model (Eq. 1), where the foliage is assumed randomly distributed, and assuming an ellipsoidal distribution of the leaf inclination using look-up-table techniques (Knyazikhin et al. 1998, described in more detail in the manual of CanEye 2006).

The gap fraction $P_0(\theta_v, \varphi_v)$ in direction (θ_v, φ_v) is related to the contact frequency by

$$P_0(\theta_v, \varphi_v) = e^{-N(\theta_v, \varphi_v)} = e^{-G(\theta_v, \varphi_v)LAI/\cos(\theta_v)} \quad (1)$$

where $N(\theta_v, \varphi_v)$ is the mean number of contacts between a light beam and a vegetation element in the direction (θ_v, φ_v) , and $G(\theta_v, \varphi_v)$ is the projection function, i.e. the mean projection of a unit foliage area in direction (θ_v, φ_v) .

The “true” LAI (LAI_{true}) is related to LAI_{eff} through the clumping index λ_0 (Chen & Black 1992), which depends both on plant structure (foliage distribution), canopy structure, and size and shape of leaves (Eq. 2).

$$LAI_{eff} = \lambda_0 LAI_{true} \quad (2)$$

In CanEye, the clumping index is computed using the Lang & Yueqin (1986) logarithm gap fraction averaging method.

2.3 Simulation of the impact of camera set-up on estimates of gap fraction

5 experimental approaches were used to test the impact of observer variability during hemispherical photography on estimates of gap fraction and LAI. Images for further analysis in CanEye were created in the experiment “Transect” only.

1. “Transect”: images were simulated using at 10 camera locations along a transect through the forest canopy.

2. “Focus”: the aperture of the camera (infinitesimal pinhole) located at the image centre was enlarged to the following values (mm): 1, 5, 10, 50, 100 to simulate the impact of lack of focus in estimates of gap fraction from digital hemiphotos.

3. “Plane”: the plane of the camera located in the image centre was tilted away from the horizontal by the following angles (degrees): 5°, 10°, 15°, 20°, 25°. This is to simulate the impact of not having a totally level camera in estimating gap fraction from digital hemiphotos.

4. “Clone”: the “camera” was randomly located within the modelled forest stand for each ray cast and the average gap fraction was calculated. This allows calculation of the ‘forest-average’ gap fraction, which is the ‘true’ gap fraction from a photon transport point of view. That measured from hemispherical photography is a sample of the true value which will obviously be a function of the specific location from where the photograph was taken.

5. “Clone Threshold”: the same setup as in the previous case, but in this case a threshold distance away from the tree coordinates in the forest stand was specified. In reality, photographs are not taken with the camera immediately adjacent to a tree trunk, and this will act to bias the gap fraction estimates somewhat. Various thresholds distances of 100, 150 and 200 cm were used.

3 RESULTS

3.1 CanEye Analyses of hemispherical images

In the following we present results of the simulations and the hemispherical image analyses for the 5 years and 9 years old forest stands only, because the simulations for older forest stands were still processing. Results of the analyses of the simulated images are presented in figures 5 and 6. Estimates of LAI_{57} , LAI_{eff} and LAI_{true} are presented in table 1.

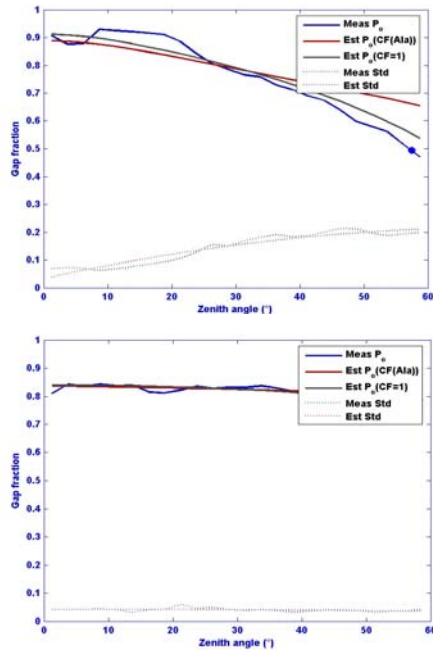


Figure 5. Gap probability as a function of view zenith angle for 9 years canopy. CanEye analyses was carried out for “thresholded” in-situ hemispherical photographs (above) and for “thresholded” simulated images (below).

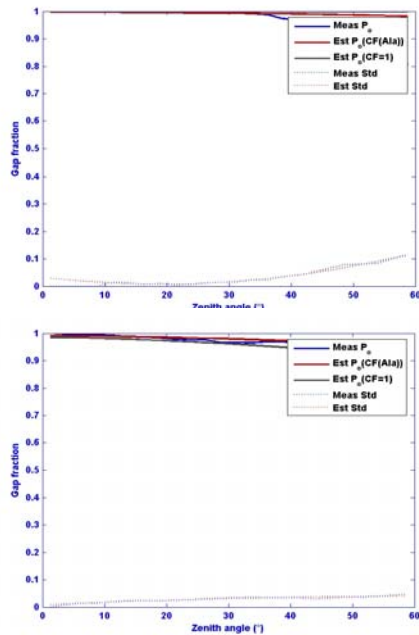


Figure 6. Gap probability as a function of view zenith angle for 5 years canopy. CanEye analyses was carried out for “thresholded” in-situ hemispherical photographs (above) and for “thresholded” simulated images (below).

Images	LAI57	LAI _{eff}	LAI _{true}
5yr, modelled	0.052	0.1	0.07
5y, measured	0.21	0	0.03
9yr, modelled	0.3	0.26	0.29
9yr, measured	0.76	0.6	1.4

Table 1: Estimates of LAI57, LAI_{eff}, and LAI_{true} derived from simulations of hemispherical reflectance within forest stands and from in-situ photographs. Results are shown for 5 years and 9 years old forest stands only.

Experiment	GP mean \pm sd
“Transect” – 5 yrs	0.88 \pm 0.05
“Focus” – 5 yrs	0.49 \pm 0.33
“Plane” – 5 yrs	0.91 \pm 0.01
“Clone_thresh” – 5 yrs	0.88 \pm 0.00
“Clone” – 5 yrs	0.88
“Transect” – 9 yrs	0.39 \pm 0.02
“Focus” – 9 yrs	0.09 \pm 0.11
“Plane” – 9 yrs	0.28 \pm 0.00
“Clone_thresh” – 9 yrs	0.39 \pm 0.02
“Clone” – 9 yrs	0.35

Table 2: Impact of choice of camera location, camera attitude and camera focus on estimates of gap fraction (mean values \pm 1 standard deviation) derived from hemispherical photography in five and nine years old modelled forest stands. The experiment “clone” calculates the average of randomly located measurements within the model forests.

4. DISCUSSION

Results from figures 5 and 6 show that gap fraction estimated from the 3D model canopies compares reasonably well with estimates derived from hemispherical photography in the 5 years and 9 years old modelled Sitka forest stands. However, it can be seen that gap probability did not decrease with increasing viewing angle for the simulated forest stands in the same way as seen in the real forest stands. This might be due to structural discrepancies between modelled and real forest stands. It may also be due to the fact that for angles beyond around 70° in the hemiphotos, the distortion in the projected field of view becomes large, whereas there is effectively no distortion in the simulated images.

4.1 Impact of camera set-up on estimates of gap fraction

Simulated variation in camera focus caused high variability in estimates of gap probability, while tilt angle had far less impact on estimates of gap probability (Table 2). Sampling design had an additional impact on gap probability estimates. The assignment of the camera to randomly chosen points within the forest can result in camera locations immediately beside a tree trunk, resulting in much lower (mean) estimates of gap probability than would be encountered in practice, where one would avoid taking photographs from within a metre or so of a tree trunk. However, any such avoidance will act to bias the resulting estimates of gap probability to be lower than the true values. This problem will tend to increase as forest stands are older/denser and the stem area density increases. In very dense plantation stands (see figure 1) it can be difficult in practice to find suitable spaces in which to place the camera and operator.

5. CONCLUSIONS

Research on techniques and algorithms for accurately and efficiently monitoring and measuring photosynthetic activity and LAI especially of forest stands has a longstanding history (Jonckheere et al. 2004, Weiss et al. 2004). While EO data have been used increasingly to derive biophysical parameters of land surfaces, dynamic structural models for forest growth have been used to improve the reliability of quantitative parameter estimation from such satellite images (Woodhouse & Hoekman 2000, Saich et al. 2003, Disney et al. 2006).

Tree growth models have been introduced to provide statistical information about dimensions and angular distributions of scattering components of forest stands that, in turn, can be used as an input to a backscatter model to predict backscatter from forest stands exploring relationships between EO data, forest structure, and biophysical parameters. 3D models are the most detailed models of this type, as they are able to proscribe the size and location of all scattering elements in the canopy. This allows them to be used for making detailed simulations of the canopy radiation regime (Widlowski et al. 2006).

Yet, a number of parameters underlying 3D structural models are unavailable or difficult to obtain. We show that digital hemispherical photography can be used to validate structural accuracy of 3D forest models generated via the tree growth model *Treegrow*. Estimates of gap probability derived from simulations of the detailed 3D structural models compared well with estimates derived from upward-looking digital hemispherical photography acquired in Sitka spruce canopies in England at least for 5 and 9 years old forest stands. However, we also found an increasing discrepancy between estimates of gap fraction (and percentage of vegetation / non-vegetation pixels in the image) for modelled and real forest stands with increasing forest age (results not shown, experiments still running). Such disagreements can be used to inform improvement of the structural models.

Age related changes in leaf structure may affect productivity of the forest, which should be manifested in the reflectance signal (see Widlowski et al. 2004, citing Caylor 2004). In upcoming experiments, we will investigate the effect of leaf structure and leaf density as well as of other structural parameters of the forest (e.g. branching traits) on the reflectance signal.

The results presented here are also relevant for generating field protocols necessary for accurate use of fisheye lens cameras to estimate LAI, as well as for testing the validity of theoretical assumptions underlying those measurements in the field. A quasi-random distribution of locations for acquiring photographs in a forest (camera locations certain distances from existing trees) is often applied in the field. This is introducing potential bias acting to reduce gap probability and LAI estimates from the resulting digital hemiphotos, especially when estimating gap probability as a function of increasing viewing zenith angle. Camera focus has the greatest impact on gap fraction probability estimates by impeding the correct classification of pixels to vegetation / non-vegetation. However, in practice this is not likely to vary as much as we have simulated here. But clearly, pixel resolution (number of pixels), and focus can have a large impact on the resulting estimates of gap fraction. Many

cameras will auto-focus on a point at infinity, but it is not clear in a dense forest canopy that this is ideal in that the lower branches of the canopy will be quite close to the camera, and as a result will be out of focus. It is these branches that will have the greatest impact on reducing gap probability, and so it is of greatest importance to get these branches into focus.

In summary, we show that it is possible to compare measured and modelled tree structure through the analysis of simulated canopy images and derived gap fraction. We also show that 3D tree models can be used very effectively to explore the impact of errors and assumptions when deriving canopy structural parameters from digital hemiphotography.

References

- Carrara A, Kowalski AS, Neirynek J, Janssens IA, Yuste JC & Ceulemans R. (2003) Net ecosystem CO₂ exchange of mixed forest in Belgium over 5 years. *Agricultural and Forest Meteorology* **119**: 209-227.
- Caylor K.K., Dowty P.R., Shugart H. H. & Ringrose S. (2004) Relationship between small-scale structural variability and simulated vegetation productivity across a regional moisture gradient in southern Africa. *Global Change Biology* **10**: 374-382.
- Chandler J. W. & Dale J. E. (1990) Needle growth in Sitka spruce (*Picea sitchensis*): effects of nutrient deficiency and needle position within shoots. *Tree Physiology* **6**: 41-56.
- Chen J. M. & Black T. A. (1992) Defining leaf area index for non-flat leaves, *Plant Cell Environ.* **15**: 421-429.
- Deng F., Chen J. M., Plummer S. (2006) Algorithm for Global Leaf Area Index Retrieval Using Satellite Imagery. *IEEE Transactions on Geoscience and Remote Sensing* **44**: 2219-2229.
- Disney M, Lewis P & Saich P. (2006) 3D modelling of forest canopy structure for remote sensing simulations in the optical and microwave domains. *Remote Sensing of Environment* **100**: 114-132.
- Dixon RK, Brown S, Houghton RA, Solomon AM et al. (1994) Carbon pool and flux of global forest ecosystems. *Science* **263**: 185-190.
- Fassnacht K. S., Gower S. T., Norman J. M., et al. (1994) A comparison of optical and direct methods for estimating foliage surface-area index in forests. *Agricultural and Forest Meteorology* **71**: 183-207.
- Jonckheere I., Fleck S., Nackaerts K., et al. (2006) Review of methods for in situ leaf area index determination. Part I. theories, sensors, and hemispherical photography. *Agricultural and Forest Meteorology* **121**: 19-35.
- Knyazikhin Y., Martonchik J. V., Diner D. J., Myneni R. B. et al. (1998) Estimation of vegetation canopy leaf area index and fraction of absorbed photosynthetically active radiation from atmosphere-corrected MISR data. *Journal of Geophysical Research* **103**: 239-256.
- Leersnijder R. P. (1992) PINOGRAM: a pine growth area model. PhD thesis, Wageningen Agricultural University, The Netherlands.
- Lewis P. (1999) Three-dimensional plant modelling for remote sensing simulation studies using the botanical plant modelling system. *Agronomie - Agriculture and Environment* **19**: 185-210.
- Magid A., Rotman S. R. & Weiss A. M. (1990) Comment on "Picture Thresholding Using an Iterative Selection Method". *IEEE Transactions on Systems, Man and Cybernetics* **20**: 1238-1239.

- Myneni R. B., Ramakrishna R. N. & Running S. W. (1997) Estimation of Global Leaf Area Index and Absorbed PAR Using Radiative Transfer Models. *IEEE Transactions on Geoscience and Remote Sensing* **35**: 1380-1393.
- Myneni R. B., Hoffman S., Knyazikhin, Y., Privette J. L. et al. (2002) Global products of vegetation leaf area and fraction absorbed PAR from year one of MODIS data. *Remote Sensing of Environment* **83**: 214-231.
- Oevelen van PJ & Woodhouse I. H. (1996) NOPEX-FOREST-DYNAMO Ground data collection and data analysis report. Report # 70. Department of Water Resources, Wageningen Agricultural University.
- Pinty B., Lavergne T., Dickinson R. E., Widlowski J. L., et al. (2006) Simplifying the interaction of land surfaces with radiation for relating remote sensing products to climate models. *Journal of Geophysical Research* **111**: 1-20.
- Price J. C. (1993) Estimating Leaf Area Index from Satellite Data. *IEEE Transactions on Geoscience and Remote Sensing* **31**: 727-734.
- Reich P. B. & Bolstad P. (2001) Productivity of evergreen and deciduous temperate forests. In: Roy J., Saugier B., Mooney H. A. (eds) *Terrestrial Global Productivity. Physiological Ecology*. Academic Press, San Diego, pp 245-283.
- Ridler T. W. & Calvard E. S. (1978) Picture thresholding using an iterative selection method. *IEEE Transactions on Systems, Man and Cybernetics* **8**: 629-632.
- Ross J. (1981) *The radiation regime and architecture of plant stands.*, Dr. W. Junk. The Hague.
- Saich P., Disney, M. I., Lewis, P. et al. (2003) Development of architectural vegetation growth models for remote sensing applications. Final report ESA contract 14940, pp 183-187.
- Schulze E. D., Lloyd J., Kelliher F. M., Wirth, C. et al. (1999) Productivity of forests in the Eurosiberian boreal region and their potential to act as a carbon sink a synthesis. *Global Change Biology* **5**: 703-722.
- Sellers P. J., Los S. O., Tucker C. J. et al. (1994) A 1x1km NDVI dataset for global climate studies. Part 2: The generation of global fields of terrestrial biophysical parameters from the NDVI. *International Journal of Remote Sensing* **15**: 3519-3545.
- Stenberg P., Linder S., Smolander H., et al. (1994) Performance of the LAI-2000 Plant Canopy Analyzer in estimating leaf-area index of some Scots pine stands. *Tree Physiology* **14**: 981-995.
- Warren-Wilson J. (1963) Estimation of foliage denseness and foliage angle by inclined point quadrats, *Aust. J. Bot.* **11**: 95-105.
- Weiss M., Baret F., Smith G. J., Jonckheere I. & Coppin B. (2004) Review of methods for in situ leaf area index (LAI) determination Part II. Estimation of LAI, errors, and sampling. *Agricultural and Forest Meteorology* **121**: 37-53.
- Widlowski J. L., Pinty, B., Gobron, N. et al. (2004) Canopy structure parameters derived from multi-angular remote sensing data for terrestrial carbon studies. *CLIMATIC CHANGE* **67**: 403-415.
- Widlowski J. L., Pinty B., Lavergne T., et al. (2006) Horizontal radiation transport in 3-D forest canopies at multiple spatial resolutions : Simulated impact on canopy absorption. *Remote Sensing of Environment* **103**: 379-397.
- Woodhouse I. H. & Hoekman D. H. (2000) Radar modelling of coniferous forest using a treegrowth model. *International Journal of Remote Sensing* **21**: 1725-1737.